Available online at www.sciencedirect.com
ScienceDirect
Bioorganic & Medicinal Chemistry Letters 17 (2007) 2197–2202
Bioorganic & Medicinal Chemistry Letters

Predicting anti-HIV activity of PETT derivatives: CoMFA approach

V. Ravichandran* and R. K. Agrawal

Pharmaceutical Chemistry Research Laboratory, Department of Pharmaceutical Sciences, Dr. H. S. Gour Vishwavidyalaya, Sagar, MP 470 003, India

Received 29 October 2006; revised 18 December 2006; accepted 23 January 2007
Available online 4 February 2007

Abstract—HIV-1 (Human Immunodeficiency Virus Type-1) is the pathogenic retrovirus and causative agent of AIDS. HIV-1 RT is one of the key enzymes in the duplication of HIV-1. Inhibitors of HIV-1 RT are classified as NNRTIs and NRTIs. NNRTIs bind in a region not associated with the active site of the enzyme. Within the NNRTIs category, there is a set of inhibitors commonly referred to as phenyl ethyl thiazolyl thiourea (PETT) derivatives. The present 3D QSAR study attempts to explore the structural requirements of phenyl ethyl thiazolyl thiourea (PETT) derivatives for anti-HIV activity. Based on the structures and biodata of previous PETT analogs, 3D-QSAR (CoMFA) study has been performed with a training set consisting of 60 molecules, which resulted in a reliable computational model with $q^2 = 0.657$, $S_{PRESS} = 0.957$, $r^2 = 0.938$, and standard error of estimation (SEE) = 0.270 with the number of partial least square (PLS) components being 5. It is shown that the steric and electrostatic properties predicted by CoMFA contours can be related to the anti-HIV activity. The predictive ability of the resultant model was evaluated using a test set comprised of 11 molecules and the predicted $r^2 = 0.893$. This model is a more significant guide to trace the features that really matter especially with respect to the design of novel compounds.

HIV-1 (Human Immunodeficiency Virus Type-1) is the pathogenic retrovirus and causative agent of AIDS or AIDS- related complex (ARC).[1,2] When viral RNA is translated into a polypeptide sequence, it is assembled in a long polypeptide chain, which includes several individual proteins, namely, reverse transcriptase, protease, integrase, etc. Before these enzymes become functional, they must be cut from the longer polypeptide chain.

Acquired immune deficiency syndrome (AIDS) is a formidable pandemic that is still wreaking havoc worldwide. The catastrophic potential of this virally caused disease may not have been fully realized. The causative moiety of the disease is human immunodeficiency virus (HIV), which is a retrovirus of the lentivirus family.[3] The three viral enzymes: reverse transcriptase, protease, and integrase encoded by the gag and gag-pol genes of HIV play an important role in the virus replication cycle. Among them, viral reverse transcriptase (RT) catalyzes the formation of proviral DNA from viral RNA, the key stage in viral replication. Its central role in viral replication makes RT a prime target for anti-HIV therapy.[4]

Two main categories of HIV RT inhibitors have been discovered to date. The first category of inhibitors is nucleoside analogs (e.g., AZT, 3TC, ddI, ddC) and the second category of inhibitors is nonnucleoside analogs. Nevirapine, delaviridine, and efavirenz are the only nonnucleoside reverse transcriptase inhibitors (NNRTI) that have received regulatory approval with several NNRTIs (MKC442, Troviridine, S-1153/ AG1549. PNU142721, ACT, and HBY1293/GW420867X) currently undergoing clinical trials. Efavirenz was the first potent anti-HIV drug to be approved by FDA and studies have shown that efavirenz penetrates into the cerebrospinal fluid, a common viral sanctuary. The therapeutic efficacy of the drug is mainly restricted due to the development of viral resistance associated with mutations that include K103N, L1001, and Y188L.[5] Comparative molecular field analysis (CoMFA) and Comparative molecular similarity indices analysis (CoMSIA) are powerful and versatile tools to build and design an activity model (QSAR) for a given set of molecules in rational drug design and related applications.[6–17]

Keywords: Anti-HIV; PETT Derivatives; 3D QSAR; CoMFA.
* Corresponding author. E-mail: phravi75@rediffmail.com

0960-894X/$ - see front matter © 2007 Elsevier Ltd. All rights reserved.
doi:10.1016/j.bmcl.2007.01.103

In the present work, we have taken 71 compounds and their anti-HIV activity from the reported work.[18,19] Many of these compounds inhibited wild type HIV-1 with ED_{50}'s between 0.001 μM and 0.005 μM in MT-4 cells. One of these thiourea derivatives troviridine showed good anti-HIV activity (0.02 μM, in clinical trial) with low cytotoxicity for MT4 cells.[19] The standard deviation of biological activity and the structural difference between the compounds are more. It insists to select these series of compounds for our 3D QSAR study. All the anti-HIV activities used in the present study were expressed as $pED_{50} = -\log_{10} ED_{50}$. Where ED_{50} is the micromolar concentration of the compounds producing 50% reduction in the cytopathic effect caused by the virus stated as the means of at least two experiments. ED_{50} values were assessed by XTT assays.[20] The compounds which were not showing confirmed anti-HIV activity in the above-cited literature have not been taken for our study. Based on the reported work,[21] we carried out molecular modeling analysis and established a 3D-QSAR model (CoMFA) to guide further structural optimization and predict the potency and physiochemical properties of clinical drug candidates.

CoMFA is a powerful and established tool for building 3D-QSAR models that can be applied to drug design.[22,23] Consequently, we used the structures of 71 PETT analogs and their anti-HIV activities (ED_{50} in μM) in MT-4 cells (Table 1) to establish CoMFA model in the present study. Sixty compounds constituted as a training set and eleven PETT analogs were used in the test set. Three-dimensional structure building and all the modeling were carried out using the SYBYL 6.7 (sgi work station) program package and conformations of compounds in the training and test sets were generated using the systematic conformational search method implemented in SYBYL 6.7.[24] Energy minimization was effected using the Tripos force field with a distance-dependent dielectric and the Powell conjugate gradient algorithm with a convergence criterion of 0.001 kcal/mol. Partial atomic charges were calculated using the Gasteiger-Huckel method.[25]

Molecular alignment was effected with the SYBYL function of 'field fit alignment method' (Figure 1). After consistently aligning the molecules within the lattice that extended 4 Å units beyond the aligned molecules in all directions with a grid step size of 2 Å, a probe sp^3 carbon atom with +1 net charge and van der Waals radius of 1.52 Å was employed. 3D QSAR models were built

Table 1. Summary of CoMFA models with 60 PETT compounds

PLS statistics	*SE*	*S*	*E*
q^2	0.657	0.398	0.451
S_{PRESS}	0.957	1.518	1.223
r^2	0.938	0.715	0.836
SEE	0.270	0.488	0.352
F	147.66	87.85	118.27
PLS components	5	4	5
Steric	0.436		
Electrostatic	0.564		

S, steric field; *E*, electrostatic field; SEE, standard error of estimation; *F*, variance ratio significant at 99% level.

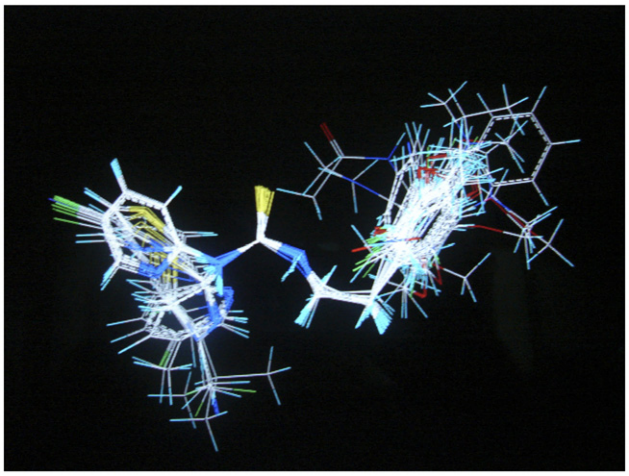

Figure 1. Field fit alignment of PETT derivatives.

by field fit alignment method in SYBYL. Steric and electrostatic interactions between the probe and the remaining molecules were calculated. The generated steric and electrostatic fields were scaled by the CoMFA-STD method in SYBYL 6.7 with a default energy of 30 kcal/mol. Electrostatic interactions were modeled using a Coulomb potential and van der Waals interactions using a Lennard-Jones potential. The regression analysis was carried out using the partial least-squares (PLS) method and cross-validation was performed using leave-one-out method with 2 kcal/mol column filter. The final model was developed with an optimum number of components yielding the highest q^2.

Cross-validated q^2 usually serves as the quantitative measurement for the prediction of CoMFA. However, Cho and Tropsha have reported that the q^2 value is sensitive to the orientation of aligned molecules on the computer terminal and, thus, might vary with the orientation by as much as 0.5 q^2 units.[26] Therefore, suitable alignment rules must be framed while constructing 3D-QSAR models. Consequently, the PETT compounds in Table 1 were aligned according to their common sub structure- compound 58 (Table 1), one of the most promising analogs in the inhibition of HIV-1 (III_B) replication in MT-4 cells, was used as the alignment template. The optimal number of components obtained is then used to derive the final QSAR model using all the compounds (without cross-validation). The conventional r^2 is used to measure the quality of the model.

To derive 3D-QSAR models, the CoMFA descriptors were used as independent variables and the pED_{50} activity value as a dependent variable. Partial least-squares (PLS) regression analyses were conducted with standard implementation in the SYBYL package. The predictive ability of the models was evaluated by leave-one-out (LOO) cross-validation. The cross-validated correlation coefficient, q^2, was calculated using Eq. 1.

$$r^2_{CV} = 1 - \frac{\sum_{i=1}^{N}(y_{exp} - y_{pred})^2}{\sum_{i=1}^{N}(y_{exp} - y_m)^2} \quad (1)$$

Table 2. Structures of PETT analogs, their anti-HIV activity in MT-4 cell lines, and their predicted activity by CoMFA

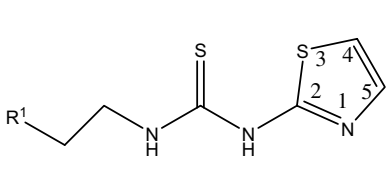

Compound 1- 25

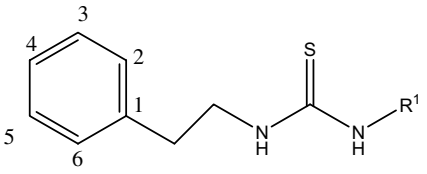

Compound 26-38

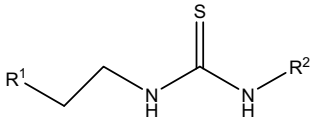

Compound 39-46

Compound	R^1	R^2	pED_{50} (μM)	
			Experimental[b]	Predicted
1	Phenyl	—	−0.1139	−0.072
2	2-Fluorophenyl	—	1	0.76
3[a]	3-Fluorophenyl	—	0.6021	1.039
4	4-Fluorophenyl	—	−0.5185	−0.424
5[a]	2-Methoxyphenyl	—	0.3979	0.915
6	3-Methoxyphenyl	—	0.2218	0.188
7	4-Methoxyphenyl	—	−0.7404	−0.801
8	2-Methylphenyl	—	0.0227	−0.039
9	2-Nitrophenyl	—	−0.0414	0.328
10	2-Hydroxyphenyl	—	−0.602	−0.051
11	2-Chlorophenyl	—	0.3979	0.211
12	3-Ethoxyphenyl	—	0.8239	0.711
13	3-Propoxyphenyl	—	−0.3424	−0.283
14[a]	3-Isopropoxyphenyl	—	0.3979	0.322
15	3-Phenoxyphenyl	—	−0.4471	−0.354
16	2,6-Dimethoxyphenyl	—	1.0457	1.181
17	2,5-Dimethoxyphenyl	—	0.3979	0.577
18	3-Bromo-6-methoxyphenyl	—	1.301	0.993
19	2-Fluoro-6-methoxyphenyl	—	0.5229	0.553
20[a]	2-Ethoxy-6-fluorophenyl	—	0.6989	1.286
21	2,6-Difluorophenyl	—	1.6989	1.381
22	2-Chloro-6-fluorophenyl	—	1.301	1.02
23	2-Pyridyl	—	−0.1139	0.092
24	3-Pyridyl	—	−0.8062	−0.491
25	2-Furyl	—	−0.716	−0.108
26	4-Methylthiazol-2-yl	—	0.3979	−0.17
27	4-Ethylthiazol-2-yl	—	0.1549	0.061
28	4-Propylthiazol-2-yl	—	−0.2041	−0.192
29	4-Isopropylthiazol-2-yl	—	−0.1139	−0.134
30[a]	4-butylthiazol-2-yl	—	−0.1139	0.093
31	4-Cyanothiazol-2-yl	—	0.6989	0.585
32	4-(Trifluoro methyl)thiazol-2-yl	—	0.301	0.515
33	4-(Ethoxy carbonyl)thiazol-2-yl	—	0.301	0.343
34	5-Chlorothiazol-2-yl	—	−0.4314	−0.373
35	1,3,4-Thiazol-2-yl	—	−0.7243	−0.496
36	2-Pyridyl	—	0.6989	0.630
37	5-Bromo-2-pyridyl	—	1.301	1.323
38	5-Methyl-2-pyridyl	—	0.8239	0.97
39[a]	2,6-Difluorophenyl	4-Cyano thiazoly-2-yl	1.5229	1.603
40	2,6-Difluorophenyl	5-Bromo-2-pyridyl	2	1.853
41	2,6-Difluorophenyl	5-Methyl-2-pyridyl	2	1.992
42[a]	2-Ethoxy-6-fluorophenyl	5-Methyl-2-pyridyl	0.6989	0.933
43	2-Ethoxy-6-fluorophenyl	5-Bromo-2-pyridyl	1.6989	1.091
44	2-Pyridyl	5-Methyl-2-pyridyl	0.5228	0.621
45	2-Pyridyl	5-Bromo-2-pyridyl	1.6989	0.938
46	2,6-Difluorophenyl	4-Ethylthiazol-2-yl	1.0969	1.478

[a]Test set compounds.
[b]The experimental ED_{50} values (in micromolar) were converted into $-\log ED_{50}$ (pED50, in micromolar). Taken from Refs. 18 and 19.

$$\text{PRESS} = \sum_{i=1}^{N} (y_{\text{exp}} - y_{\text{pred}})^2 \qquad (2)$$

where y_{exp} is the activity for training set compounds, y_{m} is the mean observed value, corresponding to the mean of the values for each cross-validation group, and y_{pred} is the predicted activity for y_{exp}.

The total set of compounds was initially divided randomly into two groups as training and test set, having 60 compounds in training set and 11 compounds in the test set. Test and training set compounds were chosen manually such that low, moderate, and high activity compounds were present approximately in equal proportions in both sets. Training set compounds were used to develop the CoMFA model and the test set compound used to validate the developed model.

We developed three CoMFA models, the first model is having both steric and electrostatic fields, the second model is having only steric field, and the third model is constructed by only electrostatic field. Finally, the model generated by combining the steric and electrostatic fields was selected as the best CoMFA model because of its statistical significance and predictive power, and the contours were analyzed using this model. The statistical parameters of the models are given in Table 1. The predicted activities are listed in Tables 2 and 3.

For the selected CoMFA model, the cross-validated r^2 (q^2) value of the training set was 0.657 with five principal components. The non-cross-validated r^2 value was 0.938 with standard error of estimation (SEE) 0.270 and covariance ratio (F) of 147.66 (significant at 99% level). The correlation between experimental activity (EA) and predicted activity (PA) is shown in Figure 2. The CoMFA model was externally validated with test set of compounds. The squared correlation coefficient (r^2 between EA and PA) value of validation set was 0.893 with standard error of estimation (SEE) 0.261. These results authenticate the good prediction ability of this 3D QSAR model.

Table 3. Structures of PETT analogs, their anti-HIV activity in MT-4 cell lines, and their predicted activity by CoMFA

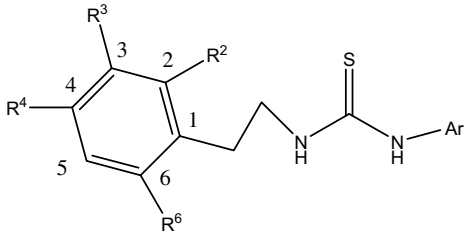

Compound 47-69

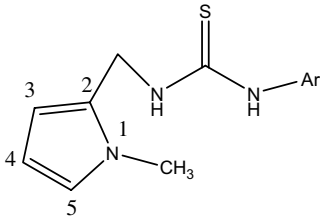

Compound 70 & 71

Compound	R^2	R^3	R^4	R^6	Ar	pED_{50}(μM)	
						Experimental[b]	Predicted
47	F	$(CO)N(Me)_2$	H	F	5-Bromo-2-pyridyl	1.0969	0.908
48	F	CH_2NAc	H	F	5-Bromo-2-pyridyl	0.0457	−0.424
49	F	CN	H	F	5-Chloro-2-pyridyl	2.2218	2.485
50	F	$N(Me)_2$	H	F	5-Chloro-2-pyridyl	1.3979	1.585
51[a]	F	$N(Me)_2$	H	F	5-Bromo-2-pyridyl	1.3979	1.367
52	F	OCH_3	H	F	5-Bromo-2-pyridyl	1.8239	1.837
53[a]	F	OC_2H_5	H	F	5-Bromo-2-pyridyl	2.2218	2.041
54	F	CH_2OCH_3	H	F	5-Bromo-2-pyridyl	2.2218	2.032
55	Cl	OC_2H_5	H	F	5-Bromo-2-pyridyl	2.1549	1.954
56	Cl	OC_2H_5	H	F	5-Chloro-2-pyridyl	2.0969	2.016
57	Cl	OC_2H_5	H	F	5-Iodo-2-pyridyl	1.8239	1.807
58	Cl	OC_2H_5	H	F	5-Cyano-2-pyridyl	2.5229	2.571
59	H	OCH_3	H	OCH_3	5-Chloro-2-pyridyl	1.3979	1.617
60	H	OC_2H_5	H	OC_2H_5	5-Bromo-2-pyridyl	1.7447	1.795
61	F	H	H	OC_2H_5	5-Bromo-2-pyridyl	1.886	1.873
62	F	F	H	OC_2H_5	5-Bromo-2-pyridyl	2.1549	2.251
63[a]	F	F	H	OCH_3	5-Bromo-2-pyridyl	2.1589	2.029
64	F	OCH_3	H	OCH_3	5-Chloro-2-pyridyl	2.6989	2.436
65	F	OC_2H_5	H	OCH_3	5-Chloro-2-pyridyl	2.301	2.399
66	OCH_3	OCH_3	H	F	5-Bromo-2-pyridyl	1.9208	2.08
67	F	$N(Me)_2$	H	F	5-Bromo-2-pyridyl	1.7447	1.885
68	F	CN	H	F	5-Bromo-2-pyridyl	1.886	2.002
69	Cl	OC_2H_5	Cl	F	5-Bromo-2-pyridyl	1.886	1.886
70	—	—	—	—	5-Cyano-2-pyridyl	0.959	0.667
71[a]	—	—	—	—	5-Chloro-2-pyridyl	0.602	0.752

[a]Test set compounds.

[b]The experimental ED_{50} values (in micromolar) were converted into $-\log ED_{50}$ (pED50, in micromolar). Taken from Refs. 18 and 19.

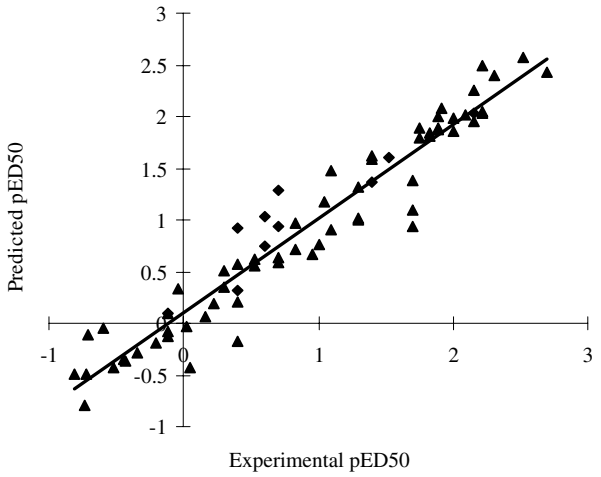

Figure 2. Correlation between experimental and predicted activities of CoMFA model. ▲ indicates training set compounds and ♦ indicates test set compounds of PETT derivatives in CoMFA model.

In the CoMFA model, the steric and electrostatic field contributions are 0.436 and 0.564, respectively. The contour maps of this model shown in Figure 3 illustrate clearly the steric and electrostatic interaction in CoMFA model. In the contour maps electrostatically favorable region corresponds to red areas and unfavorable region corresponds to blue areas. The red region near the 3rd substitution position of ethyl phenyl ring of PETT derivative suggests that biological activity can be enhanced by introduction of more electronegative groups at this position for strong electrostatic field interactions. The blue region near 4th and 5th position of ethyl phenyl ring of PETT derivative indicates that biological activity will be decreased by electronegative group at the above-mentioned positions. More than that blue contour over ethyl group between phenyl ring and thiourea suggests that biological activity will be diminished by introduction of electronegative groups at this site. Green contour near 2nd position of ethyl phenyl ring and 6th position of pyridyl ring of PETT derivative indicates that the bulky groups at this position will increase activity. Yellow contour near the 5th and 6th position of ethyl phenyl ring and 2nd and 5th position in pyridyl ring of PETT derivative indicates that bulky substituents at these positions decrease anti-HIV activity.

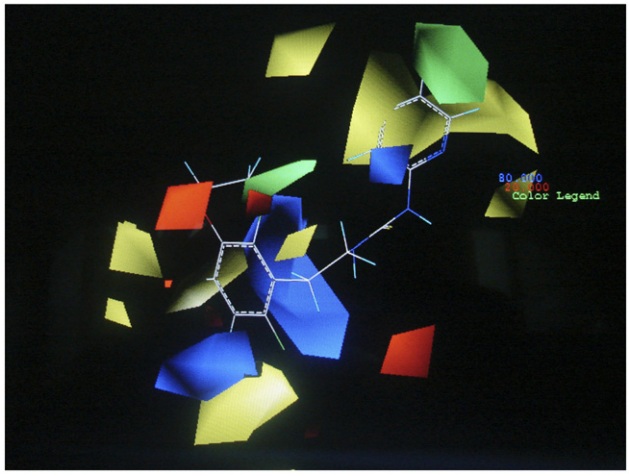

Figure 3. CoMFA contour maps for steric and electrostatic field. Green contours indicate regions where bulky groups are favorable to activity, whereas yellow contours indicate regions where bulky groups are not desirable for activity. Blue contours indicate regions where the positive groups could increase activity, whereas red contours indicate the regions needing negative charge.

The presence of electron withdrawing group like CN, F, Br, Cl, CH_3 at 5th position of 2-pyridyl ring and 2nd position of ethyl phenyl ring is conducive to anti-HIV activity. But the same groups present in 4th position of ethyl phenyl ring are detrimental to activity. The presence of bulky electronegative groups at 3rd position of ethyl phenyl ring is conducive to anti-HIV activity.

A ligand-based approach is used in rational drug design to build activity models which provide important information on possible improvements in ligand structure to increase activity. In the present study, we constructed a satisfactory 3D QSAR model of PETT derivatives using CoMFA method based on the field fit molecular alignment. The CoMFA QSAR model shows that the steric and electrostatic parts contribute equally to the activity. The contour maps from CoMFA provide useful insight into designing novel compounds with increased anti-HIV activity.

In conclusion, our current studies have established a reliable CoMFA model indicating that substituted (2nd position) ethyl-2-phenyl ring, substituted (5th position) 2-pyridyl ring, and ethyl linker between phenyl and thiourea part of the molecules are important for anti-HIV activity, which can efficiently guide further modification of PETT analogs. Based on the above-mentioned CoMFA model, we designed some new PETT derivatives, and synthesis of the designed compounds is in progress.

Acknowledgments

We would like to thank Prof. B. Suresh, Principal, J.S.S. College of Pharmacy, Ooty (TN), India, for providing access to the computational resources and extend our thanks to Prof. S. Sankar and Mr. B. R. Prashantha Kumar for their valuable help during the modeling studies. One of the authors V. Ravichandran is thankful to AICTE (QIP) for providing fellowship for this work.

References and notes

1. Gallo, R. C.; Salahuddin, S. Z.; Popovic, M.; Shearer, G. M.; Kaplan, M.; Haynes, B. F.; Palker, T. J.; Redfield, R.; Oleske, J.; Safai, B. *Science* **1984**, *224*, 500.
2. Barre-Sinoussi, F.; Chermann, J. C.; Rey, F.; Nugeyre, M. T.; Chamaret, S.; Gruest, J.; Dauguet, C.; Axler-Blin, C.; Vezinet-Brun, F.; Rouzioux, C.; Rozenbaum, W.; Montagnier, L. *Science* **1983**, *220*, 868.

3. De Clercq, E. *J. Med. Chem.* **1995**, *38*, 2491.
4. Milton, J.; Slater, M. J.; Bird, A. J.; Spinks, D.; Scott, G.; Price, C. E.; Downing, S.; Green, D. V. S.; Madar, S.; Bethell, R.; Stammers, D. K. *Bioorg. Med. Chem. Lett.* **1998**, *8*, 2623.
5. Young, S. D.; Britcher, S. F.; Tran, L. O.; Payne, L. S.; Lumma, W. C.; Lyle, T. A.; Huff, J. R.; Anderson, P. S.; Olsen, D. B.; Carroll, S. S. *Antimicrob. Agents Chemother.* **1995**, *39*, 2602.
6. Klebe, G.; Abraham, U.; Mietzner, T. *J. Med. Chem.* **1994**, *37*, 4130.
7. Bohm, M.; Sturzebecher, J.; Klebe, G. *J. Med. Chem.* **1999**, *42*, 458.
8. Buolamwini, J. K.; Assefa, H. *J. Med. Chem.* **2002**, *45*, 841.
9. Nair, A. C.; Jayatilleke, P.; Wang, X.; Miertus, S.; Welsh, W. J. *J. Med. Chem.* **2002**, *45*, 973.
10. Pungpo, P.; Hannongbua, S. *J. Mol. Graphics Modell.* **2000**, *18*, 581.
11. Jayatilleke, P. R. N.; Nair, A. C.; Zauhar, R.; Welsh, W. J. *J. Med. Chem.* **2000**, *43*, 4446.
12. Barreca, M. L.; Carotti, A.; Chimirri, A.; Monforte, A. M. *Bioorg. Med. Chem.* **1999**, *7*, 2283.
13. Hilgeroth, A.; Fleischer, R.; Wiese, M.; Heinemann, F. W. *J. Comput. Aided Mol. Design* **1999**, *13*, 233.
14. Debnath, A. K. *J. Med. Chem.* **1999**, *42*, 249.
15. Raghavan, K.; Buolamwini, J. K.; Fesen, M. R.; Pommier, Y.; Kohn, K. W. *J. Med. Chem.* **1995**, *38*, 890.
16. Oprea, T. I.; Waller, C. L.; Marshall, G. R. *Drug Des. Discovery* **1994**, *12*, 29.
17. Debnath, A. K.; Jiang, S.; Strick, N.; Lin, K.; Haberfield, P. *J. Med. Chem.* **1994**, *37*, 1099.
18. Bell, F. W.; Cantrell, A. S.; Hogberg, M.; Jaskunas, S. R.; Johansson, N. G.; Jordan, C. L.; Kinnic, M. D.; Lind, P.; Morin, J. M.; Noreen, R.; Oberg, B.; Palkowitz, J. A.; Parrish, C. A.; Pranc, P.; Sahlberg, C.; Ternansky, R. J.; Vasileff, R. T.; Vrang, L.; West, S. J.; Zhang, H.; Zhou, X. X. *J. Med. Chem.* **1995**, *38*, 4929.
19. Cantrell, A. S.; Engelhardt, P.; Hogberg, M.; Jaskunas, S. R.; Johansson, N. G.; Jordan, C. L.; Kinnic, M. D.; Lind, P.; Morin, J. M.; Noreen, R.; Oberg, B.; Palkowitz, J. A.; Parrish, C. A.; Pranc, P.; Sahlberg, C.; Ternansky, R. J.; Vasileff, R. T.; Vrang, L.; West, S. J.; Zhang, H. *J. Med. Chem.* **1996**, *39*, 4261.
20. Weislow, O. S.; Kiser, R.; Fine, D. L.; Bader, J.; Shoemaker, R. H.; Boyd, M. R. *J. Nat. Cancer Inst.* **1989**, *81*, 577.
21. Chen, H. F.; Yao, X. J.; Li, Q.; Yuan, S. G.; Panaye, A.; Doucet, J. P.; Fan, B. T. *SAR QSAR Environ. Res.* **2003**, *14*, 455.
22. Chen, H. F.; Li, Q.; Yao, X. J.; Fan, B. T.; Yuan, S. G.; Panaye, A.; Doucet, J. P. *QSAR Comb. Sci.* **2003**, *22*, 604.
23. Chen, H. F.; Li, Q.; Yao, X. J.; Fan, B. T.; Yuan, S. G.; Panaye, A.; Doucet, J. P. *QSAR Comb. Sci.* **2004**, *23*, 36.
24. SYBYL [computer program]. Version 6.7. St. Louis (MO): Tripose Assosiciates, USA.
25. Clark, M.; Cramer, R. D., III; Opdenbosch, N. V. *J. Comput. Chem.* **1989**, *10*, 982.
26. Cho, S. J.; Tropsha, A. *J. Med. Chem.* **1995**, *38*, 1060.